

A Mathematical Approach for Optimizing Dendritic Cell-Based Immunotherapy

Gennady Bocharov, Neville J. Ford, and Burkhard Ludewig

Summary

Adoptive dendritic cell (DC)-based immunotherapy represents a promising approach to overcome peripheral tolerance against autologous tumor antigens and to maintain protective antitumor immunity. The translation of successful preclinical studies, however, appears to be hampered by new complexities associated with the clinical situation. Mathematical modeling provides the means for qualitative and quantitative analysis, predictions for complex dynamic systems in immunology, and for the design and improvement of therapeutic approaches. We present here a workable computational methodology for developing meaningful data- and hypothesis-driven mathematical models for DC-based immunotherapy with a particular focus on numerical parameter estimation and sensitivity analysis.

Key Words: Mathematical model; immune response; computer simulation; data fitting; parameter estimation; sensitivity analysis; predator–prey dynamics; dendritic cell; cytotoxic T-lymphocyte; numerical software.

1. Introduction

Immunotherapeutic approaches based on adoptive transfer of dendritic cells (DC) expressing relevant antigens may be used for active mobilization of cellular immune responses (cytotoxic T-lymphocytes [CTL], T-helper cells, and natural killer [NK] cells) against tumors (1,2). The efficacy of this active immunization depends on the complex biology of the DC life cycle and their interaction with T-cells. The kinetics of this interaction and its sensitivity to relevant parameters are still incompletely understood. These parameters include antigen loading, DC maturation stage, frequency and route of DC injection, frequency and activation status of T-cells, and the homing rate of DC to and their persistence within lymphoid tissues. Mathematics provides the means for an integrative description of simplified models of various immunological phenomena, including those arising in the context of adoptive immunotherapy. Its primary role is to assist in parameter estimation (e.g., the cellular interaction kinetic rates, life spans, delays, activation thresholds) and analysis (the “numbers game”), and to make testable predictions in advance of experiments and clinical applications.

From: *Methods in Molecular Medicine*, vol. 109: *Adoptive Immunotherapy: Methods and Protocols*
Edited by: B. Ludewig and M. W. Hoffmann © Humana Press Inc., Totowa, NJ

Table 1
Decision Making Before and During the Modeling Process ^a

| |
|---|
| Modeling objectives |
| Determine the focus of the investigation. <ul style="list-style-type: none">• General understanding of the rules underlying the observed behavior (e.g., causality inferences and/or critical parameters of system dynamics)• Reliable calculations of system dynamics• Specific predictions about new observations—experimental design• Characterize and analyze the data |
| Modeling approaches |
| Decide on the approach to develop the model. <ul style="list-style-type: none">• Building block (models are formulated by applying the governing physical laws/constraints and constitute relations to the subsystems)• Black box (models are formulated on the basis of the input-output characteristics of the system, no consideration of its internal functioning) |
| Model types |
| Decide on the types of equations that provide the appropriate compromise between simplicity and tractability on the one hand, and accuracy on the other. <ul style="list-style-type: none">• Continuous in time• Discrete in time• Deterministic• Stochastic |
| Types of building block models |
| <ul style="list-style-type: none">• Microscopic (spatially distributed)• Macroscopic (lumped) |

^a Summarized from **refs. 3–5**

Mathematical modeling involves a number of distinct steps. In order to establish a mathematical model, many simplifying assumptions have to be specified and decisions must be made, either explicitly or implicitly (3–5) (Table 1). The translation process, starting from a particular (immunological) phenomenon and ending in a mathematical formalism (i.e., a set of equations), is the hardest part of applying mathematics, because it involves the conversion of imprecise assumptions into formulas. We describe here one possible approach to modeling the interaction of DC with CTL. In the presented model, the DC–CTL interaction is described by adapting different theoretical frameworks, such as predator–prey models from population biology (6) and Monod-type kinetics with saturation which are applied in biochemistry (7). We are considering these deterministic models at the macroscopic level of the whole immune system, and neglect details such as spatial structures of lymphoid organs or cytokine networks. The overall aim of this approach is to produce a scientifically meaningful mathematical model that is both descriptive and predictive.

In the “Methods” section we explain the use of the computational techniques for *in silico* simulations, using the models, parameter estimation, information-theoretical assessment of the mathematical model given the data, and sensitivity analysis. These represent the major aspects of the general problem of valid inference (8). Although our main interest has been the mathematical modeling of the population dynamics of DC–CTL interaction in mice, the computational methodology has widespread applicability. To describe the kinetics of the population densities of immune cells, we utilize either ordinary or delay differential (in the case of memory effects) equations, which describe the rate of change of cell population densities as a function of time t .

2. Materials

2.1. Experimental Data

Reliable input from experimental or clinical research in terms of precise and comprehensive datasets is a core part of an interdisciplinary modeling approach. The data set presented in **Table 2** was generated using established protocols (9,10). Briefly, major histocompatibility complex (MHC) class I tetramers complexed with the immunodominant CTL epitope (gp33) derived from the glycoprotein of the lymphocytic choriomeningitis virus (LCMV-GP) (11) were used to follow activation of gp33-specific CTL after immunization with DC. DC derived from transgenic mice ubiquitously expressing the first 60 aa of LCMV-GP including gp33 (H8-DC) (12) were injected intravenously (i.v.) into naïve C57BL/6 recipient mice. At the indicated time points following immunization, the densities of the following cell populations as a function of time t were determined:

- “Activated” $\text{CD8}^+\text{CD62L}^-$ T-cells staining with the gp33-tetramer (tet^+) in spleen that have downregulated the CD62L molecule, $E_a(t)$
- “Quiescent” $\text{CD8}^+\text{CD62L}^+\text{tet}^+$ cells in spleen $E_m(t)$.

Furthermore, to assess the availability of adoptively transferred DC for productive interaction with T-cells within secondary lymphoid organs, ^{51}Cr -labeled H8-DC were injected i.v. into naïve recipient mice, and the accumulated radioactivity was determined in spleen at different time points using established protocols (13). The data set for homing of adoptively transferred DC from blood to spleen has been published elsewhere (14).

2.2. Simulation Software

The practical way to study mathematical models is based on using numerical techniques to approximate the solutions. To understand the DC–CTL interaction dynamics, model equations were evaluated under different parameter settings—a “direct” approach. Differential equations of the model were programmed using the universal computer language FORTRAN. Efficient and reliable software packages such as MATLAB (Website: <http://www.mathworks.com>) or Berkeley Madonna (Website: <http://www.berkeleymadonna.com>) represent more convenient alternatives to the “classical” programming approach, because they automate a number of steps (e.g., programming of equations, selection of the numerical method) of the process of solving initial value problems for ordinary or delay differential equations.

Table 2
Example of the Original Data Set (Mean \pm Standard Deviation) for the Kinetics
of tet⁺ CD8 T-Cells Expansion Induced after Intravenous (i.v.) Injection of 2×10^5 H8-DC^a

| Days after i.v. injection | Splenocytes (cells) | CD8 ⁺ T-cells | tet ⁺ CD8 T-cells | % CD62L ⁻ | Derived data used for fitting of the model variable | |
|------------------------------|------------------------------|------------------------------|---------------------------------|----------------------|--|--|
| | | | | | E_a (activated gp33- specific CTL) | $E_a + E_m$ (total gp33- specific CTL) |
| d4 | $(7.0 \pm 0.66) \times 10^7$ | $(1.0 \pm 0.02) \times 10^7$ | $(1.4 \pm 0.19) \times 10^5$ | $43 \pm 6.7 \%$ | 1.4×10^5 | — |
| d7 | $(4.0 \pm 1.5) \times 10^7$ | $(7.0 \pm 2.7) \times 10^6$ | $(3.6 \pm 1.8) \times 10^5$ | $82 \pm 5.6 \%$ | 3.6×10^5 | — |
| d12 | $(6.1 \pm 0.67) \times 10^7$ | $(6.1 \pm 0.71) \times 10^6$ | $(1.7 \pm 0.55) \times 10^5$ | $71 \pm 8.2 \%$ | — | 1.7×10^5 |
| d18 | $(5.5 \pm 0.73) \times 10^7$ | $(5.1 \pm 1.2) \times 10^6$ | $(6.6 \pm 1.3) \times 10^4$ | $49 \pm 5.2 \%$ | — | 6.6×10^4 |

^a The data set used for fitting the model predictions for activated cytotoxic T-lymphocytes (CTL) (E_a) and the total CTL ($E_a + E_m$) variables of the mathematical model.

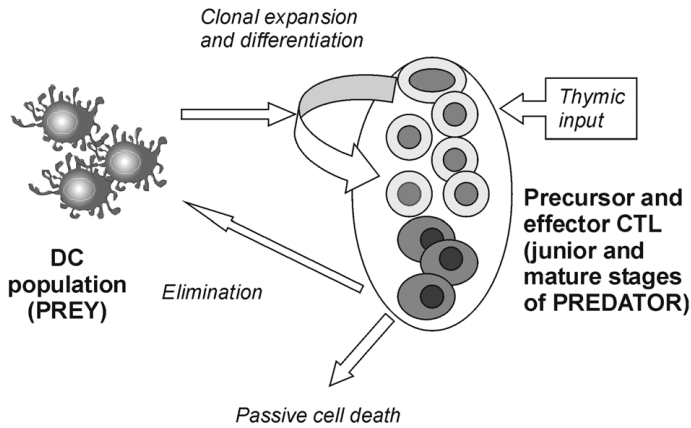


Fig. 1. Conceptual model for the predator–prey type induction/regulation of $CD8^+$ T-cell responses by dendritic cells (DC). Antigen-expressing DC migrate from blood to spleen, where they induce clonal expansion of naïve antigen-specific cytotoxic T-lymphocytes (CTL), whereas activated CTL eliminate DC. Arrows indicate the modeled processes.

3. Methods

3.1. Generation of a Conceptual Scheme (Model) of the System

The first task in a data- and hypothesis-driven modeling approach is to choose/specify the functional form of the model to represent the data of the system under analysis (3). Although many variables and parameters might seem necessary to describe the effect of DC on CTL, one must *a priori* restrict the model to the most important interactions. We quote from Burnham and Anderson (8): “Development of the *a priori* set of candidate models often should include a global model: a model that has many parameters, includes all potentially relevant effects, and reflects causal mechanisms thought likely, based on the science of situation.” This type of a global model for a systemic dynamics of DC–CTL interaction has recently been developed by Ludewig et al. (14). Our conceptual model is based on the spatio-temporal view of the organization and predator–prey type regulation of $CD8^+$ T-cell responses by DC *in vivo*. Antigen-expressing DC migrate irreversibly from blood to the spleen, where they induce clonal expansion of naïve antigen-specific CTL. Activated CTL eliminate the DC and recirculate among spleen, blood, and peripheral tissues. The key element of the model is the predator–prey-type interaction of DC with antigen-specific CTL (Fig. 1). We present here our modeling methodology for the splenic compartment of the immune system.

3.2. Specifying Assumptions and Selecting Quantities

To formulate equations for DC–CTL interaction following i.v. injection, we make the following simplifying biological assumptions. Such a list is also helpful for the evaluation of the modeling results from the viewpoint of the underlying biology.

1. DC do not re-circulate from lymphoid organs into the blood after intravenous injection (15).
2. Adoptively transferred DC are in mature state (10).
3. DC-mediated induction of antigen-specific CTL is due to their interaction in the spleen (14).
4. DC do not divide in secondary lymphoid organs (16).
5. DC decay due to a short life span (17) and their killing by activated CTL (9,18).
6. The population of antigen-specific CTL in spleen is split into quiescent (naïve or central memory-like) and activated CTL (effector or effector memory-like) (19).
7. CTL re-circulate among spleen, blood, and peripheral organs (e.g., liver).

The required quantities for the specific model depend on the conceptual scheme and the assumptions. The quantities include here time as an independent variable, time-dependent variables (population densities of cells), and the parameters that characterize the kinetics of the specified processes. The biological meaning and units of the parameters considered in the presented model of DC–CTL interaction are listed in **Table 3**.

3.3. Derivation of Model Equations

The cell population dynamics can be represented by the following prototype mass balance equation (see **Note 1**):

Change rate of number of cells of j -th type at time $t =$

\pm transfer between compartments + cell division – cell death \pm transition between states (1)

We model the localized population dynamics of DC–CTL interaction, i.e., in the spleen, and ignore the DC re-circulation between spleen and blood.

The rate of change in the density of DC in the spleen is modeled as:

$$\frac{d}{dt} D(t) = \mu_{BS} \cdot \frac{Q_{Blood}}{Q_{Spleen}} \cdot D_{Blood}(t) - \alpha_D \cdot D(t) - b_{DE} \cdot E_a(t) \cdot D(t) \quad (2)$$

The first term represents the trafficking of DC from blood to spleen (Q_{Blood} and Q_{Spleen} being the volumes of the blood and spleen compartments, respectively), and the other two take into account the natural death of the cells and their elimination by activated CTL. We substitute the formulae identified in (14) for the kinetics of DC in the blood $D_{Blood}(t)$.

The dynamics of activated CTL is modeled by the following equation:

$$\frac{d}{dt} E_a(t) = \alpha_{E_a} \cdot [E^{naive} - E_a(t)] + b_p \cdot \frac{D(t - \tau_d) \cdot E_a(t - \tau_d)}{\theta_D + D(t - \tau_d)} - r_{am} \cdot E_a(t) + b_a \cdot D(t) \cdot E_m(t) \quad (3)$$

The first term considers the homeostasis of naïve CTL in the spleen, the second term represents the DC-induced division of CTL proceeding at the rate that saturates at a high number of DC. The time lag between the cognate interaction of CTL with DC represents the duration of “preprogramming” of CTL for division and differentiation (20). The last two terms take into account the silencing of activated CTL into quiescent “memory” cells (third term) and the activation of the memory cells by DC.

Table 3
Parameters of the DC-CTL Model in Spleen

| Notation | Biological Definition | Estimate (units) [99% Confidence Interval] |
|--|---|--|
| μ_{BS} | Transfer rate of H8-DCs from blood to spleen | 2.832 d^{-1} |
| $t_{1/2} = \ln 2 / \alpha_D$ | Half-life of gp-33-expressing DC | 3 d (ad hoc fixed value) |
| b_{DE} | Per capita elimination rate of H8-DCs by activated CTL | $0.487 \times 10^{-5} \text{ mL/cell/d}$ [0.13×10^{-6} , 0.6×10^{-5}] |
| E^{naive} | The number of naïve gp-33-specific CTL contributing to primary clonal expansion | 370 cells (ad hoc fixed value) |
| τ_d | Duration of antigen preprogrammed CTL divisions | 1 d (ad hoc fixed value) |
| $t_{1/2}^{E_a} = \ln 2 / \alpha_{E_a}$ | Half-life of activated CTL | 5.78 d [0.12, $+\infty$) |
| $t_{1/2}^{E_m} = \ln 2 / \alpha_{E_m}$ | Half-life of resting “memory” CTL | 69 d (ad hoc fixed value) |
| b_p | Maximal expansion factor of activated CTL per d | 12 d^{-1} [10, 85] |
| θ_D | DC density in the spleen for half-maximal proliferation rate of CTL | $2.12 \times 10^3 \text{ cell/mL}$ [7.5×10^2 , 1.2×10^4] |
| r_{am} | Fraction of activated CTL reverting into resting “memory” cells per day | 0.01 d^{-1} [0.4×10^{-3} , 1.2] |
| b_a | Activation rate of quiescent CTL by DCs | $10^{-3} \text{ mL/cell/d}$ |

The equation for the dynamics of quiescent “memory” CTL is:

$$\frac{d}{dt}E_m(t) = r_{am} \cdot E_a(t) - [\alpha_{E_m} + b_a \cdot D(t)] \cdot E_m(t) \quad (4)$$

which considers the transition of the activated CTL into the quiescent “memory” state, the death of *memory* CTL at some slow rate, and the activation of memory CTL depending on the availability of DC.

3.4. Computer Simulation of the System Dynamics

A typical computer simulation includes the following steps:

1. Program the set of differential equations of the model, either following protocols specified in specialized simulation packages (*see Methods*) or using universal computer languages such as FORTRAN or C++.
2. Set initial values for the time-dependent population densities of DC and CTL.
3. Set the values for the model parameters (*see Note 2* for an example of how to derive the initial guess for CTL proliferation parameters b_p , θ_D).
4. Set run-time parameters—the start and finish times as well as the report times for the solution and the error-per-step tolerance in the solver.

There are several difficulties in obtaining efficiently a numerical approximation to the solution of the model equations (*see Note 3*). It follows that the computer simulations require specification of values for the model parameters. The parameter values can be obtained from experimental data sets either directly, or using special numerical procedures for the “inverse” modeling approach.

3.5. Estimation of Parameters and Confidence Intervals Via Data-Fitting

Estimation of adjustable parameters of a mathematical model with specified architecture is another central task of data-driven modeling (3). The purpose of data-fitting is to calculate values of the model parameters that optimize some objective function which is a measure of the fit (agreement) between the simulated values (predictions of the model) and the data (*see Note 4*). **Figure 2** shows the experimental data and the corresponding best-fit solution of the mathematical model.

3.5.1. Least-Squares Fitting Functions

Let the set of observation times $\{t_j\}_{j=1}^N$ and observations $\{y_j^i\}_{j=1}^N$ for M ($1 \leq i \leq M$) of the model variables be specified. An example of the experimental data set representing the kinetics of tet⁺ CD8 T-cells expansion after i.v. injection of 2×10^5 H8-DC used in parameter estimation is given in **Table 2**. Simulation of the system with the model suggests prediction (a regression function) for the observed variable $y^i(t_j, \mathbf{p})$, which depends on the adjustable parameters \mathbf{p} , i.e., the model parameter vector with L components. The common ordinary least-squares (LSQ) error measure of the match between the model and data is given by the objective function determined by the square of the absolute deviation between the model and data:

$$\Phi(\mathbf{p}) = \sum_{j=1}^N \sum_{i=1}^M [y_j^i - y^i(t_j, \mathbf{p})]^2 \quad (5)$$

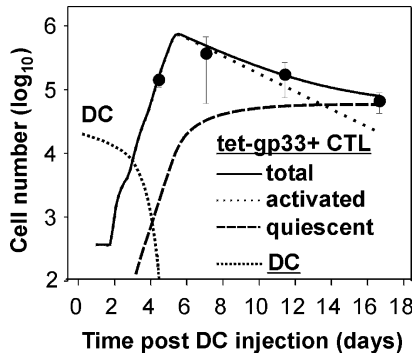


Fig. 2. Data vs model description for the population dynamics of dendritic cells (DC) and cytotoxic T-lymphocytes (CTL) in spleen induced by intravenous injection of 2×10^5 gp33-presenting H8-DC. The symbols represent averages of 3 mice \pm standard deviation. The smooth lines predict the population dynamics of the total tet⁺, activated tet⁺, and quiescent memory tet⁺ CTLs and H8-DCs for the best-fit estimates of the model parameters. DC elimination follows a biphasic kinetics; the first, slower phase reflects their life parameters. DC elimination results from the killing effect by activated CTLs.

The weighted LSQ objective function

$$\Phi(\mathbf{p}) = \sum_{j=1}^N \sum_{i=1}^M w_j^i \left[y_j^i - y^i(t_j, \mathbf{p}) \right]^2 \quad (6)$$

can be used when different weights have to be given to particular observations. A natural choice for the weights could be the inverse variances $w_j^i = (\sigma_j^i)^{-2}$ of the observations. The LSQ approach proves to be efficient when the variation in scale of the data set over the observation time interval is within one order of magnitude. This is exactly the case with the data for the initial biodistribution kinetics of DC after intravenous injection (*see* **ref. 14** and **Note 5**).

3.5.2. Minimization of the Least-Squares Function

The numerical technique for finding the best-fit parameter estimates for a given data set, mathematical model, and objective function requires (1) providing an initial guess for the model parameters; (2) solving the model equations to compute $\Phi(\mathbf{p})$; and (3) adjusting the parameter values by some minimization routine available, for example, in the MATLAB library (`fmin`). Because the parameters of the model are constrained to be nonnegative, we used a \log_{10} -transformation for the parameters, so that the resulting sequence of reduced order data-fitting problems were treated as an unconstrained minimization (*see* **Note 6**).

There are software packages such as Berkeley Madonna that can automatically find the values of a number of parameters in a model that minimize the deviation between the model's output and a data set. In principle, these facilities greatly enhance the capability of treating the parameter estimation problem. However, data-fitting with non-linear differential equations-based models is a type of expertise that can be learned only in actual practice (*see refs. 21–23* for extensive discussion of various aspects of statistical techniques and computational methods).

3.5.3. Computation of Confidence Intervals

To characterize the precision or reliability of best-fit parameter estimates (\mathbf{p}^*) a number of approaches exist, of which we consider (1) the variance-covariance matrix for estimated parameters (23); and (2) the profile-likelihood-based method (24) (*see Note 7*). Alternatively, a bootstrap approach may be used (21,25). The confidence interval analysis is a computation-intensive procedure. The simplest approach is to approximate the 95% confidence intervals using estimates of the standard errors $p_*^l \pm 1.96\sigma_l$, where $\sigma_l = \sqrt{v_{ll}}$, $1 \leq l \leq L$ stand for the diagonal elements of the variance-covariance matrix. In turn, the matrix elements are determined via the residual sum of LSQ function, the number of degrees of freedom, and the Hessian matrix (22,23), according to the formula

$$\begin{bmatrix} v_{11} & c_{12} & c_{13} & \cdots & c_{1L} \\ c_{21} & v_{22} & c_{23} & \cdots & c_{2L} \\ c_{31} & c_{32} & v_{33} & \cdots & c_{3L} \\ \cdots & \cdots & \cdots & \cdots & \cdots \\ c_{L1} & c_{L2} & c_{L3} & \cdots & v_{LL} \end{bmatrix} = 2 \frac{\Phi(\mathbf{p}_*)}{N_{obs} - L} \begin{bmatrix} \frac{\partial^2}{\partial p_1^2} \Phi(\mathbf{p}_*) & \frac{\partial^2}{\partial p_1 \partial p_2} \Phi(\mathbf{p}_*) & \frac{\partial^2}{\partial p_1 \partial p_3} \Phi(\mathbf{p}_*) & \cdots & \frac{\partial^2}{\partial p_1 \partial p_L} \Phi(\mathbf{p}_*) \\ \frac{\partial^2}{\partial p_2 \partial p_1} \Phi(\mathbf{p}_*) & \frac{\partial^2}{\partial p_2^2} \Phi(\mathbf{p}_*) & \frac{\partial^2}{\partial p_2 \partial p_3} \Phi(\mathbf{p}_*) & \cdots & \frac{\partial^2}{\partial p_2 \partial p_L} \Phi(\mathbf{p}_*) \\ \frac{\partial^2}{\partial p_3 \partial p_1} \Phi(\mathbf{p}_*) & \frac{\partial^2}{\partial p_3 \partial p_2} \Phi(\mathbf{p}_*) & \frac{\partial^2}{\partial p_3^2} \Phi(\mathbf{p}_*) & \cdots & \frac{\partial^2}{\partial p_3 \partial p_L} \Phi(\mathbf{p}_*) \\ \cdots & \cdots & \cdots & \cdots & \cdots \\ \frac{\partial^2}{\partial p_L \partial p_1} \Phi(\mathbf{p}_*) & \frac{\partial^2}{\partial p_L \partial p_2} \Phi(\mathbf{p}_*) & \frac{\partial^2}{\partial p_L \partial p_3} \Phi(\mathbf{p}_*) & \cdots & \frac{\partial^2}{\partial p_L^2} \Phi(\mathbf{p}_*) \end{bmatrix}^{-1} \quad (7)$$

where N_{obs} and L stand for the total number of scalar observations and the number of model parameters, respectively. The Hessian matrix can be approximated using the complete information matrix or via numerical differentiation provided in MATLAB.

The estimates of the parameters for DC–CTL interaction in spleen and their confidence intervals are shown in **Table 3** (*see Note 7*).

3.5.4. Evaluation of the Model Parsimony and Accuracy

In general, the biological model architectures are not comprehensively justified on the basis of proven mechanisms, but reflect a parsimonious characterization of the system under study (26). The mathematical model presented here is not the only plausible model for studying the dynamics of DC–CTL interaction in vivo. Other formulations may be preferable given a different context (e.g., data) or a different set of goals. It is important, therefore, not only to rank plausible models with respect to their consistency with the data (as measured by the best-fit objective function), but also to consider their distance to an unknown “true model” underlying the data set.

The information-theoretic framework provides a basis for such assessment of information complexity of the model (the model parsimony) and the selection of the best ones with respect to the information in the data (8). Using the maximized-likelihood function, one can compute the value of the corrected Akaike's information criterion (AIC) (appropriate for data sets smaller than 40 units):

$$\mu_{cAIC} = -2 \ln [\mathcal{L}(\mathbf{p}_*, \sigma)] + 2(L+1) \left[1 + \frac{L+2}{N_{obs} - (L+2)} \right] \quad (8)$$

with $\mathcal{L}(\mathbf{p}_*, \sigma)$ being the maximized likelihood function, or the revised relative indicator

$$\Delta \mu_{cAIC} = N_{obs} \ln \Phi(\mathbf{p}_*) + 2(L+1) \left[1 + \frac{L+2}{N_{obs} - (L+2)} \right] \quad (9)$$

in which extraneous terms are discarded and the relationship between the maximum-likelihood estimation and the LSQ estimation (either ordinary- or Log-LSQ) is used. The best model is considered to be that which yields the lowest value of the indicators. The indicators can be regarded as taking parsimony into account.

3.6. Sensitivity Analysis

The major advantage of a mathematical model is that the model parameters can be easily altered and the effect on system dynamics can be examined via sensitivity analysis (see **Note 8**). We present an example in which the initial numbers of injected DC and naïve CTL were changed to predict the effect on the peak expansion of CTL. In this process, the model equations were run using various combinations of the numerical values of the initial numbers of DC and CTL; other parameter values are shown in **Table 3**. The computer experiments summarized in **Fig. 3** suggest that the peak CTL expansion is a conserved feature of the DC–CTL interaction dynamics once the initial numbers of DC and CTL have reached a saturation level. Furthermore, this simulation indicates that increasing the initial number of CTL above a certain threshold does not lead to further expansion because of the accelerated elimination of the antigen-presenting DC.

4. Notes

1. Various functional forms can be suggested for process terms in the above equation, as illustrated for the DC-induced proliferation rate of T-cells in **Table 4**. To model dose-response curves, there is a broad set of phenomenological equations available that allow one to get the desired shape, including one-site saturation, sigmoidal with variable slope, four-parameter logistic equation, and so on. It has to be determined which of these forms is most consistent with the system under consideration, and this can be judged either by using *a priori* biological arguments, or by confronting against experimental data as presented, for example in (27), or using the information-theoretic model selection criteria (see **Subheading 3.5.4.**).
2. Experimental data on CTL priming with DC (10) indicate that 100–1000 DC have to reach the spleen to achieve protective levels of CTL activation. These numbers directly suggest the range for the initial estimates of the threshold parameter of half-maximal CTL activation, i.e., $100 \leq \theta_D \leq 1000$ (cells). The doubling time of CTL during the

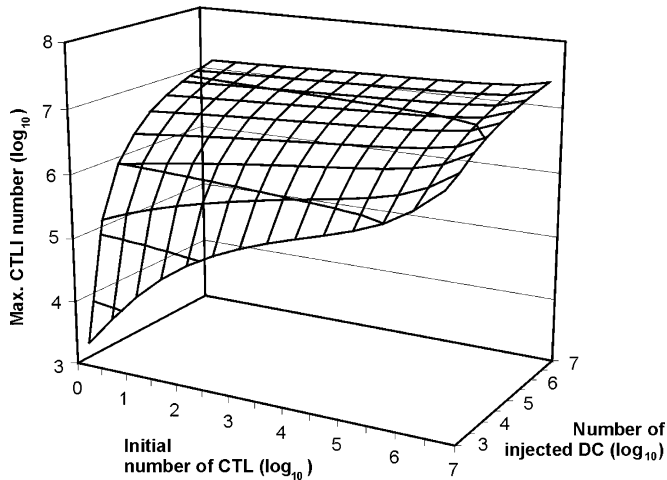


Fig. 3. Sensitivity analysis of CTL expansion to parameters variation. The maximal expansion of gp33-specific CTL as a function of the initial number of intravenously injected H8-DC and the initial number of the specific CTL.

Table 4
Some Functional Forms for DC-Induced CTL Growth
and the Associated Qualitative Implications

| Process | | | | | |
|--|-------------|-------------------------------|-------------|-----------------------------------|-------------|
| DC-induced per capita T cell division rate | | | | | |
| Form1 | Dose/Effect | Form2 | Dose/Effect | Form3 | Dose/Effect |
| $\sim DC$ | | $\sim \frac{DC}{\theta + DC}$ | | $\sim \frac{DC}{\theta + (DC)^2}$ | |

expansion phase ranges from 6 to 24 h. This suggests a plausible range for the CTL amplification per day parameter $1 \leq b_p \leq 2^4 = 16 \text{ (d}^{-1}\text{)}$. Data-fitting procedures are required to further refine these initial estimates (*see Subheading 3.5.*).

- 3. Voit (7) presents a useful practical guide to doing simulations with mathematical models formulated using systems of ordinary differential equations. They offer a basic, easy to install and start software for Power Law Analysis and Simulation (PLAS). Some differential equations model processes with widely separated decay times (called *stiff*) require special stiff solvers (based upon either implicit Runge-Kutta or Gear’s methods) to produce simulations. These are available, for example, in the software package Berkeley Madonna. In the case of models formulated with delay (rather than ordinary) differential equations, software development is still an active area of research. Some interesting guidelines and recipes on how to conduct *in silico* experiments on the model system are discussed in (7) for biochemical models.

4. We have available observations as input data, which typically arise from a multiple series of observations, in which case the individual data have to be summarized in some way (e.g., as means and standard errors). Since the basis of the data-fitting usually includes assumptions about distributions (e.g., normal or Log-normal) of the errors in observations, it is important to ensure that those assumptions are realistic. A general statistical framework is the Bayesian approach, which under some natural assumptions reduces to Maximum A Posteriori Estimation and, further down, to Maximum Likelihood (ML) Estimation (3,23). The choice depends on the knowledge of the statistical features of the data, expectations in advance about the model parameter values, and the selected set of models. If one uses a single model and assumes a uniform prior on the parameter values, then the ML approach would be the natural choice (3,23). The LSQ parameter estimation is equivalent to the ML estimation under the set of assumptions (often made implicitly) that (1) the observational errors are normally distributed, (2) equivalent positive and negative deviations from expected values differ by equal amounts; and (3) the errors between samples are independent and identically distributed. Other powers of the deviation between the model and the data can be used depending on the error distribution—for example, the first power would correspond to an exponential distribution of the errors (3).
5. Immunological characteristics may vary over several orders of magnitude. In such cases logarithmic scaling should be applied in order to make the data-fitting problem equally sensitive to differences between the model and data in the lower end of the observed values. Statistically, this implies an assumption of geometric normality of observational errors, in which equivalent deviations differ by equal proportions. Minimizing the Log-LSQ function is equivalent to maximizing the likelihood function under the assumption that the observational errors are independent and Log-normally distributed. The parameter estimation problem corresponds to a choice of Log-LSQ (relative deviation) objective function

$$\Phi_{LogLS}(\mathbf{p}) = \sum_{j=1}^N \sum_{i=1}^M \left\{ \ln(y_j^i) - \ln[y^i(t_j, \mathbf{p})] \right\}^2 \quad (10)$$

The DC-induced population dynamics of tet⁺ CD8⁺ T-cells is exactly such a case. To estimate the model parameters characterizing the DC-CTL interaction, we minimized the Log-LSQ function in an iterative way over sequentially expanding time intervals dominated by different sets of parameters.

6. In terms of efficiency, it may be advantageous to try a number (or a combination) of minimization methods. Whereas the initial estimates of model parameters can first be improved by a computationally simple, slowly converging method (e.g., derivative-free Simplex method), the resulting better guess can further be improved using a computationally extensive but rapidly converging procedure (e.g., quasi-Newton method). Good starting values for parameter estimates can sometimes be obtained by a sequential process of refining the estimates via fitting the subsets of the data, which are obtained by subdividing the observation interval. As the size of the subinterval increases, the best-fit parameter values can be improved in a step-by-step manner. The limited accuracy of the numerical solution of the mathematical model and, therefore, the correct number of digits in the value of the LSQ function must be accounted for in the minimization process, especially if it uses finite-difference approximations to the derivatives of the objective functions.
7. For complex mathematical models the variance-covariance matrix approach to assess the precision of parameter estimates is more difficult to implement because of the complexity

(this is the case for the mathematical model of systemic DC–CTL interaction). We used a different approach: approximate (e.g., 99%) confidence regions for every best-fit parameter estimate (α_*) of the whole parameter vector $\mathbf{p}_* = [\mathbf{p}_*^{(L-1)}, \alpha_*]$ were obtained using the profile-likelihood-based method (24), by searching for those values of α that satisfied the following inequality

$$\frac{\Phi_{LogLS}(\mathbf{p}_*^{[L-1]}, \alpha)}{\Phi_{LogLS}(\mathbf{p}_*^{[L-1]}, \alpha_*)} \leq e^{\frac{\chi_{1,1-0.01}^2}{N_{obs}}} \quad (11)$$

The value of $\chi_{1,0.99}^2$, which stands for the 0.99th quantile of the χ^2 -distribution on one degree of freedom is 6.635 (see standard statistical textbooks), N_{obs} stands for the number of observations. Therefore, numerically one needs to find the two extreme values of α (the endpoints of the confidence range) that enable

$$\Phi_{LogLS}(\mathbf{p}_*^{[L-1]}, \alpha) = e^{\frac{6.635}{N_{obs}}} \cdot \Phi_{LogLS}(\mathbf{p}_*^{[L-1]}, \alpha_*) \quad (12)$$

8. Sensitivity analysis in modeling of biochemical and bioengineering systems has been discussed elsewhere (7,28). To summarize, the sensitivity analysis has multiple functions: it can indicate the controllability of the system dynamics, the parameter redundancy in the model, the effect of errors in the data on parameter estimates, and the predictability of the system, as well as assisting in ranking the importance of the modeled processes. In addition to the simplest form of sensitivity analysis—i.e., how a permanent perturbation in parameter(s) around the best-fit value affects the solution (transient or steady-state)—one may study the effect of time-varying perturbation(s), or the sensitivity of more complex system features, like the clonal burst size, the transition time to a particular state, and so on. The practical details of sensitivity analysis with PLAS software created by Ferreira are discussed in detail by Voit (7). The simplest sensitivity computations require that the parameter of interest be independent of the remaining parameters in the model; otherwise one has to take into account all functional dependences upon other parameters.

Acknowledgments

We thank Hans Hengartner and Rolf Zinkernagel for continued support. This work was supported by the Swiss National Science Foundation, the Kanton of St. Gallen, the Wellcome Trust, the Alexander von Humboldt Foundation, the Leverhulme Trust, and the Russian Foundation for Basic Research.

References

1. Schuler, G., Schuler-Thurner, B., and Steinman, R. M. (2003) The use of dendritic cells in cancer immunotherapy. *Curr. Opin. Immunol.* **15**, 138–147.
2. Steinman, R. M. and Pope, M. (2002) Exploiting dendritic cells to improve vaccine efficacy. *J. Clin. Invest.* **109**, 1519–1526.
3. Gershenfeld, N. (2002) *The Nature of Mathematical Modelling*. Cambridge University Press, Cambridge, UK.
4. Kutz, M. (2002) *Standard Handbook of Biomedical Engineering and Design*. McGraw-Hill Professional Publishing, New York, NY.

5. Blanchard, P., Devaney, R. L., and Hall, G. R. (1998) *Differential Equations*. Brooks/Cole Publishing Company, Pacific Grove, CA.
6. Volterra, V. (1926) Variations and fluctuations in the numbers of co-existing animal species. In: *The Golden Age of Theoretical Biology 1923–1940*. Scudo, F. M., and Ziegler, J. R., eds. Springer, Berlin, Heidelberg, Germany, pp. 65–236.
7. Voit, E. O. (2000) *Computational Analysis in Biochemical Systems. A Practical Guide for Biochemists and Molecular Biologists*. Cambridge University Press, Cambridge, UK.
8. Burnham, K. P. and Anderson, D. R. (2002) *Model Selection and Multimodel Inference—a Practical Information-Theoretic Approach, 2nd Ed.* Springer, New York, NY.
9. Ludewig, B., Bonilla, W. V., Dumrese, T., Odermatt, B., Zinkernagel, R. M., and Hengartner, H. (2001) Perforin-independent regulation of dendritic cell homeostasis by CD8(+) T cells in vivo: implications for adaptive immunotherapy. *Eur. J. Immunol.* **31**, 1772–1779.
10. Ludewig, B., Ehl, S., Karrer, U., Odermatt, B., Hengartner, H., and Zinkernagel, R. M. (1998) Dendritic cells efficiently induce protective antiviral immunity. *J. Virol.* **72**, 3812–3818.
11. Gallimore, A., Glithero, A., Godkin, A., et al. (1998) Induction and exhaustion of lymphocytic choriomeningitis virus-specific cytotoxic T lymphocytes visualized using soluble tetrameric major histocompatibility complex class I–peptide complexes. *J. Exp. Med.* **187**, 1383–1393.
12. Ehl, S., Hombach, J., Aichele, P., et al. (1998) Viral and bacterial infections interfere with peripheral tolerance induction and activate CD8+ T cells to cause immunopathology. *J. Exp. Med.* **187**, 763–774.
13. Eggert, A. A., Schreurs, M. W., Boerman, O. C., et al. (1999) Biodistribution and vaccine efficiency of murine dendritic cells are dependent on the route of administration. *Cancer Res.* **59**, 3340–3345.
14. Ludewig, B., Krebs, P., Junt, T., et al. (2004) Determining control parameters for dendritic cell–cytotoxic T lymphocyte interaction. *Eur. J. Immunol.* **34**, 2407–2418.
15. Fossum, S. (1988) Lymph-borne dendritic leukocytes do not recirculate, but enter the lymph node paracortex to become interdigitating cells. *Scand. J. Immunol.* **27**, 97–105.
16. Ardavin, C., Martinez, del Hoyo, G., Martin, P., et al. (2001) Origin and differentiation of dendritic cells. *Trends Immunol.* **22**, 691–700.
17. Ruedl, C., Koebel, P., Bachmann, M., Hess, M., and Karjalainen, K. (2000) Anatomical origin of dendritic cells determines their life span in peripheral lymph nodes. *J. Immunol.* **165**, 4910–4916.
18. Hermans, I. F., Ritchie, D. S., Yang, J., Roberts, J. M., and Ronchese, F. (2000) CD8+ T cell-dependent elimination of dendritic cells in vivo limits the induction of antitumor immunity. *J. Immunol.* **164**, 3095–3101.
19. Wherry, E. J., Teichgraber, V., Becker, T. C., et al. (2003) Lineage relationship and protective immunity of memory CD8 T cell subsets. *Nat. Immunol.* **4**, 225–234.
20. van Stipdonk, M. J., Lemmens, E. E., and Schoenberger, S. P. (2001) Naive CTLs require a single brief period of antigenic stimulation for clonal expansion and differentiation. *Nat. Immunol.* **2**, 423–429.
21. Armitage, P., Berry, G., and Matthews, J. N. S. (2002) *Statistical Methods in Medical Research*. Blackwell Science, Oxford, UK.
22. Baker, C. T. H., Bocharov, G., Paul, C. A. H., and Rihan, F. A. (2004) Computational modeling with functional differential equations: identification, selection and sensitivity, *Appl. Num. Math.*, in press.
23. Bard, Y. 1974. *Nonlinear Parameter Estimation*. Academic, New York, NY.

24. Venzon, D. J. and Mooogavkor, S. H. (1988) A method for computing profile-likelihood-based confidence intervals. *Appl. Statistician* **37**, 87–94.
25. De Boer, R. J., Oprea, M., Antia, R., Murali-Krishna, K., Ahmed, R., and Perelson, A. S. (2001) Recruitment times, proliferation, and apoptosis rates during the CD8(+) T-cell response to lymphocytic choriomeningitis virus. *J. Virol.* **75**, 10,663–10,669.
26. Wood, S. N. and Thomas, M. B. (1999) Super-sensitivity to structure in biological models. *Proc. R. Soc. Lond. B Biol. Sci.* **266**, 565–570.
27. Borghans, J. A., Taams, L. S., Wauben, M. H., and De Boer, R. J. (1999) Competition for antigenic sites during T cell proliferation: a mathematical interpretation of in vitro data. *Proc. Natl. Acad. Sci. USA* **96**, 10,782–10,787.
28. Rabitz, H. (1981) Chemical sensitivity analysis theory with applications to molecular dynamics and kinetics. *Comput. Chem.* **5**, 167–180.



<http://www.springer.com/978-1-58829-406-7>

Adoptive Immunotherapy

Methods and Protocols

Ludewig, B.; Hoffmann, M.W. (Eds.)

2005, XVI, 500 p., Hardcover

ISBN: 978-1-58829-406-7

A product of Humana Press